Water Resources Research

Supporting Information for

Unsaturated Flow Effects on Solute Transport in Soils

Luwen Zhuang[1, 2], Amir Raoof[2], Mojtaba G. Mahmoodlu[2, 3], Sara Biekart[2], Riemer de Witte[2], Lubna Badi[2], Martinus Th. van Genuchten[2, 4], and Kairong Lin[1]

[1]School of Civil Engineering, Sun Yat-sen University, Zhuhai, China, [2]Department of Earth Sciences, Utrecht University, P.O. Box 80021, 3508 TA, Utrecht, Netherlands, [3]Department of Watershed and Rangeland Management, Gonbad Kavous University, Iran, [4]Center for Environmental Studies, São Paulo State University, UNESP, Rio Claro, SP 13506-900

Contents of this file

Introduction

This supporting information provides brief description of the gamma transmission method (Text S1), ADE transport parameters estimated from the BTCs of sands S1 and S2 at different depths (Tables S1-S6), MIM transport parameters estimated from the BTCs of sands S1 and S2 at different depths (Tables S7-S12), and ADE transport parameters obtained from the BTCs of sand S1 using the small sandbox (Table S13).

Gamma Transmission Method

Text S1.

The gamma system consisted of a radioactive source ^{241}Am, with an energy peak of 59 keV. A schematic view is shown in Figure S1. Gamma radiation attenuation in an unsaturated soil sample can be described using Beer-Lambert's equation as follows

$$I = I_0 \exp(-\mu_s l_s - \mu_w l_w) \quad \text{(S1)}$$

where I and I_0 denote measured and corresponding reference intensities, μ_s and μ_w, are the solid and water attenuation coefficients, respectively, l_s and l_w denote the overall length of the solid and water phases along the path of the gamma-ray beam, respectively.

The diameter of the gamma-ray beam was 6 mm. Measured intensities hence were average values over the cross section of the beam and the soil thickness. The attenuation coefficients μ_s and μ_w were commonly assumed linearly related to the length of the solid and water phases, respectively. The attenuation coefficients μ_s and μ_w were measured and calculated beforehand. Detailed information has been reported in the literature (Fritz, 2012). When only deionized water is present without any solute, the reference intensity I_0 was set equal to the measured intensity of the empty sandbox. For saturated samples, the total thickness of the soil sample was known as the width of the sandbox (i.e., 2 cm). The total thickness under saturated conditions is the sum of l_s and l_w. Therefore, the values of l_w and l_s=2- l_w can be calculated from the measured intensity for the saturated samples using Equation S1. Sand porosity (φ) and water saturation (S) can then be calculated as:

$$\varphi = \frac{l - l_s}{l} \text{ and } S = \frac{l_w}{l - l_s} \quad \text{(S2)}$$

respectively, in which l is the total thickness of the soil sample (i.e. 2 cm, being the width of our sandbox). For one set of solute transport experiments, the value of l_s was fixed at its value for the initial saturated sample, assuming no change of the porosity during the experiment. For each unsaturated condition, the value of l_w can be calculated based on the measured value of I.

After establishing the unit-gradient flow, the value of l_w was fixed. When the solution was applied, the variation of I was only caused by the different concentration of the solution. Equation (S2) is modified to

$$I = I_0 \exp(-\mu_s l_s - \mu_w l_w - \mu_c l_w) \quad \text{(S3)}$$

where μ_c is the attenuation coefficient of the solution, which is commonly a linear function of solute concentration (Udagani, 2013). We determined the relationship between u_c and solute concentration prior to the experiments. Under the unit-gradient flow condition, the values of u_s, l_s, u_w, and l_w were fixed. The values of μ_c can be calculated based on the variation of the intensity I. For each gamma measurement, the value of solute concentration can be derived from the value of μ_c.

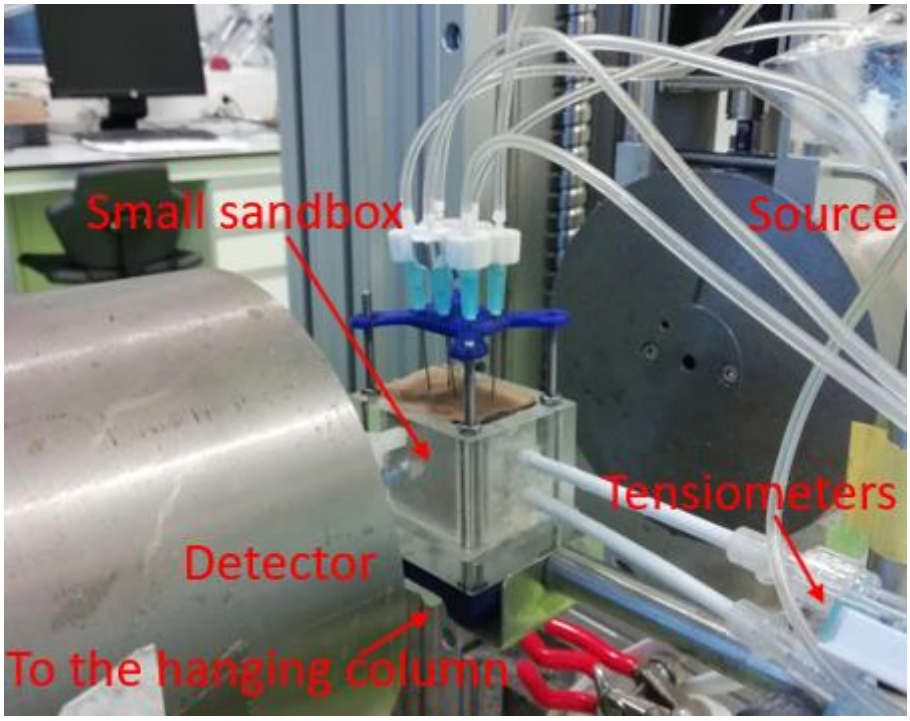

Figure S1. View of the small sandbox

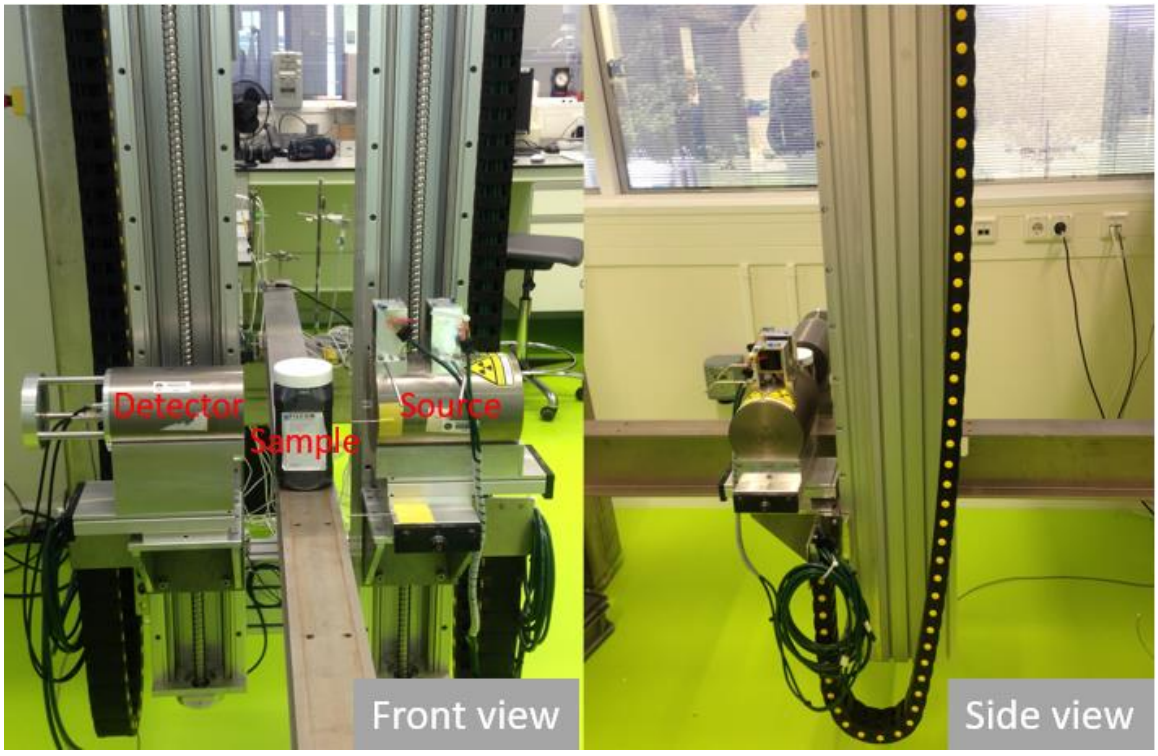

Figure S2. View of the gamma ray system used for the small sandbox BTCs

ADE transport parameters estimated from the BTCs of sands S1 and S2 at different depths

Table S1. ADE transport parameters estimated from the BTCs of sand S1 at *x*=10.5 cm.

ADE model, *x*=10.5 cm					
Exp.	*S*	*v*	*D*	*λ*	R^2
	-	cm min^{-1}	cm^2 min^{-1}	cm	-
S1L-1	1.00	0.760	0.0125	0.017	0.9869
S1L-2	1.00	0.096	0.0019	0.020	0.9328
S1L-3	0.80	0.882	0.0447	0.051	0.9992
S1L-4	0.70	0.679	0.0361	0.053	0.9996
S1L-5	0.60	0.346	0.0289	0.083	0.9989
S1L-6	0.50	0.134	0.0099	0.074	0.9990
S1L-7	0.44	0.051	0.0047	0.093	0.9828
S1L-8	0.35	0.014	0.0013	0.090	0.9964

Table S2. ADE transport parameters estimated from the BTCs of sand S1 at *x*=18.0 cm.

ADE model, *x*=18.0 cm					
Exp.	*S*	*v*	*D*	*λ*	R^2
	-	cm min^{-1}	cm^2 min^{-1}	cm	-
S1L-1	1.00	0.806	0.0132	0.016	0.9989
S1L-2	1.00	0.101	0.0018	0.018	0.9618
S1L-3	0.80	0.827	0.0576	0.070	0.9984
S1L-4	0.70	0.687	0.0466	0.068	0.9993
S1L-5	0.60	0.372	0.0333	0.089	0.9961
S1L-6	0.50	0.141	0.0161	0.114	0.9974
S1L-7	0.44	0.055	0.0071	0.128	0.9920
S1L-8	0.35	0.016	0.0020	0.128	0.9953

Table S3. ADE transport parameters estimated from the BTCs of sand S1 at *x*=25.5 cm.

ADE model, *x*=25.5 cm					
Exp.	*S*	*v*	*D*	*λ*	R^2
	-	cm min^{-1}	cm^2 min^{-1}	cm	-
S1L-1	1.00	0.813	0.0114	0.014	0.9994
S1L-2	1.00	0.103	0.0015	0.015	0.9878
S1L-3	0.80	0.792	0.0513	0.065	0.9954
S1L-4	0.70	0.667	0.0463	0.069	0.9946
S1L-5	0.60	0.351	0.0307	0.087	0.9957
S1L-6	0.50	0.135	0.0162	0.120	0.9892
S1L-7	0.44	0.055	0.0074	0.134	0.9917
S1L-8	0.35	0.016	0.0021	0.132	0.9917

Table S4. ADE transport parameters estimated from the BTCs of sand S2 at *x*=10.5 cm.

ADE model, *x*=10.5 cm

Exp.	S	v	D	λ	R^2
	-	cm min^{-1}	cm^2 min^{-1}	cm	-
S2L-1	1.00	0.173	0.007	0.042	0.9833
S2L-2	1.00	0.319	0.010	0.033	0.9992
S2L-3	0.81	7.804	0.540	0.069	0.9977
S2L-4	0.68	6.473	4.000	0.618	0.9887
S2L-5	0.58	3.417	5.063	1.482	0.9774
S2L-6	0.49	2.186	3.208	1.468	0.9855
S2L-7	0.44	0.678	0.715	1.053	0.9886
S2L-8	0.35	0.394	0.354	0.897	0.9914
S2L-9	0.30	0.216	0.218	1.012	0.9806
S2L-10	0.27	0.080	0.055	0.680	0.9894

Table S5. ADE transport parameters estimated from the BTCs of sand S2 at x=18.0 cm.

ADE model, x=18.0 cm					
Exp.	S	v	D	λ	R^2
	-	cm min^{-1}	cm^2 min^{-1}	cm	-
S2L-1	1.00	0.177	0.008	0.045	0.9806
S2L-2	1.00	0.326	0.013	0.039	0.9987
S2L-3	0.81	8.458	0.552	0.065	0.9916
S2L-4	0.68	5.518	2.431	0.441	0.9987
S2L-5	0.58	3.488	5.826	1.670	0.9787
S2L-6	0.49	2.272	2.453	1.080	0.9943
S2L-7	0.44	0.775	0.804	1.038	0.9960
S2L-8	0.35	0.411	0.352	0.858	0.9936
S2L-9	0.30	0.212	0.208	0.979	0.9882
S2L-10	0.27	0.087	0.077	0.883	0.9862

Table S6. ADE transport parameters estimated from the BTCs of sand S2 at x=25.5 cm.

ADE model, x=25.5 cm					
Exp.	S	v	D	λ	R^2
	-	cm min^{-1}	cm^2 min^{-1}	cm	-
S2L-1	1.00	0.177	0.009	0.049	0.9894
S2L-2	1.00	0.324	0.015	0.046	0.9976
S2L-3	0.81	8.550	0.638	0.075	0.9961
S2L-4	0.68	6.243	1.751	0.280	0.9954
S2L-5	0.58	3.908	2.681	0.686	0.9852
S2L-6	0.49	2.373	1.679	0.708	0.9918
S2L-7	0.44	0.862	0.682	0.792	0.9929
S2L-8	0.35	0.430	0.283	0.657	0.9956
S2L-9	0.30	0.235	0.131	0.559	0.9949
S2L-10	0.27	0.101	0.062	0.617	0.9900

MIM transport parameters estimated from the BTCs of sands S1 and S2 at different depths

Table S7. MIM transport parameters estimated from the BTCs of sand S1 at *x*=10.5 cm.

MIM model, *x*=10.5 cm							
Exp.	S	v	D	λ_m	β	ω	R^2
	-	cm min^{-1}	cm^2 min^{-1}	cm	-	min^{-1}	-
S1L-3	0.80	0.879	0.0382	0.043	0.986	4.0×10^{-3}	0.9993
S1L-4	0.70	0.677	0.0302	0.045	0.982	4.5×10^{-3}	0.9996
S1L-5	0.60	0.343	0.0239	0.069	0.981	8.2×10^{-4}	0.9992
S1L-6	0.50	0.132	0.0082	0.062	0.978	1.7×10^{-4}	0.9994
S1L-7	0.44	0.050	0.0036	0.072	0.967	8.0×10^{-5}	0.9837
S1L-8	0.35	0.014	0.0009	0.068	0.960	1.5×10^{-5}	0.9974

Table S8. MIM transport parameters estimated from the BTCs of sand S1 at *x*=18.0 cm.

MIM model, *x*=18.0 cm							
Exp.	S	v	D	λ_m	β	ω	R^2
	-	cm min^{-1}	cm^2 min^{-1}	cm	-	min^{-1}	-
S1L-3	0.80	0.820	0.0423	0.052	0.978	2.5×10^{-3}	0.9989
S1L-4	0.70	0.683	0.0279	0.041	0.962	7.2×10^{-3}	0.9998
S1L-5	0.60	0.370	0.0185	0.050	0.944	5.2×10^{-3}	0.9966
S1L-6	0.50	0.139	0.0100	0.072	0.961	2.8×10^{-4}	0.9993
S1L-7	0.44	0.054	0.0032	0.058	0.941	1.8×10^{-4}	0.9958
S1L-8	0.35	0.015	0.0012	0.078	0.953	1.8×10^{-5}	0.9974

Table S9. MIM transport parameters estimated from the BTCs of sand S1 at *x*=25.5 cm.

MIM model, *x*=25.5 cm							
Exp.	S	v	D	λ_m	β	ω	R^2
	-	cm min^{-1}	cm^2 min^{-1}	cm	-	min^{-1}	-
S1L-3	0.80	0.789	0.0391	0.049	0.980	4.6×10^{-3}	0.9926
S1L-4	0.70	0.617	0.0365	0.059	0.923	2.4×10^{-4}	0.9962
S1L-5	0.60	0.346	0.0239	0.069	0.980	2.6×10^{-4}	0.9970
S1L-6	0.50	0.126	0.0110	0.087	0.927	7.1×10^{-5}	0.9930
S1L-7	0.44	0.053	0.0040	0.075	0.954	6.6×10^{-5}	0.9967
S1L-8	0.35	0.015	0.0013	0.085	0.937	8.1×10^{-6}	0.9968

Table S10. MIM transport parameters estimated from the BTCs of sand S2 at *x*=10.5 cm.

MIM model, *x*=10.5 cm							
Exp.	S	v	D	λ_m	β	ω	R^2
	-	cm min^{-1}	cm^2 min^{-1}	cm	-	min^{-1}	-
S2L-3	0.81	7.752	0.0798	0.010	0.868	5.2×10^{-1}	0.9981
S2L-4	0.68	5.932	0.8133	0.137	0.795	6.7×10^{-2}	0.9887
S2L-5	0.58	2.814	2.4370	0.866	0.801	4.3×10^{-3}	0.9850
S2L-6	0.49	1.585	1.6720	1.055	0.721	1.3×10^{-3}	0.9893

S2L-7	0.44	0.549	0.4239	0.773	0.800	4.2×10^{-4}	0.9920
S2L-8	0.35	0.245	0.1900	0.776	0.622	5.2×10^{-5}	0.9935
S2L-9	0.30	0.118	0.0865	0.736	0.552	4.3×10^{-5}	0.9877
S1L-10	0.27	0.040	0.0217	0.540	0.501	9.4×10^{-6}	0.9653

Table S11. MIM transport parameters estimated from the BTCs of sand S2 at *x*=18.0 cm.

MIM model, *x*=18.0 cm							
Exp.	S	v	D	λ_m	β	ω	R^2
	-	cm min^{-1}	cm^2 min^{-1}	cm	-	min^{-1}	-
S2L-3	0.81	8.447	0.1859	0.022	0.881	6.9×10^{-1}	0.9916
S2L-4	0.68	5.363	0.3544	0.066	0.749	1.5×10^{-1}	0.9993
S2L-5	0.58	2.881	0.7935	0.275	0.711	1.0×10^{-2}	0.9958
S2L-6	0.49	2.133	0.5201	0.244	0.747	1.8×10^{-2}	0.9961
S2L-7	0.44	0.727	0.0542	0.074	0.650	9.2×10^{-3}	0.9970
S2L-8	0.35	0.391	0.0665	0.170	0.739	3.5×10^{-3}	0.9955
S2L-9	0.30	0.201	0.0176	0.088	0.693	1.5×10^{-3}	0.9923
S1L-10	0.27	0.083	0.0150	0.180	0.717	6.3×10^{-4}	0.9837

Table S12. MIM transport parameters estimated from the BTCs of sand S2 at *x*=25.5 cm.

MIM model, *x*=25.5 cm							
Exp.	S	v	D	λ_m	β	ω	R^2
	-	cm min^{-1}	cm^2 min^{-1}	cm	-	min^{-1}	-
S2L-3	0.81	8.514	0.1836	0.022	0.875	6.4×10^{-1}	0.9961
S2L-4	0.68	6.171	0.8514	0.138	0.900	8.5×10^{-2}	0.9934
S2L-5	0.58	3.535	0.8977	0.254	0.855	6.2×10^{-3}	0.9969
S2L-6	0.49	2.271	0.4420	0.195	0.852	1.0×10^{-2}	0.9964
S2L-7	0.44	0.823	0.1822	0.221	0.840	3.6×10^{-3}	0.9965
S2L-8	0.35	0.417	0.1093	0.262	0.872	1.6×10^{-3}	0.9965
S2L-9	0.30	0.228	0.0289	0.127	0.824	1.7×10^{-3}	0.9976
S1L-10	0.27	0.098	0.0208	0.213	0.853	3.8×10^{-4}	0.9918

ADE transport parameters obtained from the BTCs of sand S1 using the small sandbox

Table S13. ADE parameters obtained from the BTCs of sand S1 using the small sandbox

ADE model, *x*=1.5 cm					
Exp.	S	v	D	λ	R^2
	-	cm min^{-1}	cm^2 min^{-1}	cm	-
S1S-1	1.00	2.585	0.7504	0.290	0.9891
S1S-2	1.00	1.386	0.5228	0.377	0.9493
S1S-3	0.80	1.149	0.5236	0.456	0.9176
S1S-4	0.70	0.677	0.2974	0.439	0.9802

S1S-5	0.60	0.372	0.2295	0.617	0.9043
S1S-6	0.50	0.180	0.1175	0.652	0.9240
S1S-7	0.41	0.065	0.0300	0.459	0.9594
S1S-8	0.28	0.024	0.0293	1.222	0.9164

SI References

Fritz, S. (2012). Experimental investigations of water infiltration into unsaturated Soil: analysis of dynamic capillarity effects. M.S. thesis, Stuttgart Univ., Stuttgart, Germany.

Udagani, C. (2013). Dependence Of gamma ray attenuation on concentration of manganese (II) chloride solution. *International Journal of Scientific & Technology Research*, *2*(55–59).